

Foundation Model-Drive High-Confidence Electrocardiogram-Based Chagas Disease Detection

Pindong Chen¹, Bo Yu¹, Wenlong Wu¹

¹Xiaomi Health Lab, Beijing, China

Abstract

As part of the George B. Moody PhysioNet Challenge 2025, team MIWEAR developed an approach for detecting Chagas disease from 12-lead electrocardiograms (ECGs). Using ResNet-18 with five-fold cross-validation, we estimated sample confidence and curated a subset by retaining only high-confidence positives and negatives. A large-scale ECG foundation model pretrained on over ten million recordings was then fine-tuned, alongside EfficientNet-B0 and ResNet-18 trained on the curated data. Model predictions were fused by averaging. Cross-validation confirmed that confidence-based sampling improved the performance. The standalone ECG foundation model achieved a Challenge score 0.238 on the test set, ranking 10th in the final leaderboard, underscoring strong transferability under distribution shifts. These findings show that foundation models provide a reliable backbone, while fusion enhances stability, offering a competitive strategy for ECG-based Chagas disease detection.

1. Introduction

We participated in the 2025 George B. Moody PhysioNet Challenge, which invited teams to develop automated, open-source algorithms for identifying Chagas disease from electrocardiograms (ECGs) [1–3]. While serological testing is the gold standard for diagnosis, ECG-based interpretation provides a scalable and cost-effective screening alternative, particularly in resource-constrained settings.

The availability of large-scale public ECG databases, including CODE-15, SaMi-Trop, PTB-XL, REDS-II, and ELSA-Brasil [4–8], has enabled the development of data-driven approaches for this task. However, these datasets differ substantially in labeling quality, class balance, and demographic coverage. In particular, weakly labeled samples from large cohorts pose challenges for effective model training, as naive use of these data may amplify label noise.

Our team, MIWEAR, designed an approach that combines confidence-guided sample selection with deep neu-

ral networks to address these issues. Instead of discarding weakly labeled data entirely, we sought to extract reliable subsets by leveraging prediction confidence. This strategy allowed us to mitigate noise while still benefiting from the scale of large databases. We then integrated pre-trained ECG foundation models with conventional deep architectures, and employed ensembling to enhance predictive robustness.

In this paper, we describe our methodology in detail, present results from cross-validation and hidden validation evaluation, and discuss the advantages and limitations of our approach in the context of Chagas disease detection.

2. Methods

2.1. Data Preprocessing

All recordings from the training databases were first parsed into a unified metadata table containing the recording length, source, age, sex, and diagnostic label. To ensure data quality, we excluded samples shorter than 2900 samples (corresponding to approximately 7.25 s at 400 Hz).

Because the CODE-15% subset was both substantially larger than the other datasets and contained weaker labels, we applied random undersampling to reduce its prevalence in the training pool. Specifically, a fixed fraction of CODE-15% samples was retained, while all samples from the other databases were preserved. This step aimed to alleviate dataset imbalance and reduce the influence of noisy or uncertain labels.

For demographic attributes, we mapped sex into binary form (male = 1, female = 0) and retained patient age as a continuous feature. When demographic information was missing or ambiguous, we set its value to a missing indicator rather than discarding the record, in order to maximize data usage.

Each electrocardiogram (ECG) signal was then standardized into a 12-lead format (I, II, III, aVR, aVL, aVF, V1–V6). We reordered channels accordingly and discarded non-standard leads. To mitigate baseline wander and high-frequency artifacts, we applied median filtering

to each lead. Signals were subsequently resampled to 400 Hz to unify sampling frequency across databases.

After resampling, amplitudes were normalized on a per-lead basis using min–max scaling,

$$x' = \frac{x - \min(x)}{\max(x) - \min(x) + \epsilon}, \quad (1)$$

where $\epsilon = 10^{-5}$ prevents division by zero. This approach scales each lead into $[0, 1]$ while preserving inter-lead dynamics. To account for noisy outliers, we additionally replaced undefined values with zeros.

Finally, each signal was truncated or zero-padded to a fixed length of 4096 samples (≈ 10.2 s), ensuring consistent input dimensions for model training. This representation provides sufficient temporal context while controlling memory footprint. The resulting dataset consisted of a tensor with shape $(N, 12, 4096)$, accompanied by diagnostic labels and demographic covariates. To address class imbalance, we computed positive class weights as the ratio of negative to positive samples and applied them during loss calculation.

2.2. Confidence-Based Sample Selection

Label noise and heterogeneity across datasets can severely affect supervised training. To mitigate this, we used a ResNet-18 trained with five-fold cross-validation to generate probability estimates for all samples in the first stage. Let p_i denote the probability of sample i being positive. The selection criteria were:

$$t_+ = Q_5(p), \quad t_- = Q_{95}(p) \quad (2)$$

$$P = \{i \mid y_i = 1, p_i \in [t_+, 1]\} \quad (3)$$

$$N = \{j \mid y_j = 0, p_j \in [0, t_-]\} \quad (4)$$

$$N_{final} = 95 \times P \quad (5)$$

where Q_{95} and Q_5 are the 95th and 5th percentiles of the distribution of predicted probabilities. P and N are the selected positive and negative samples. To balance the dataset, the number of final negatives $|N|$ was chosen as $95 \times |\mathcal{P}|$. This procedure ensured that the curated subset contained only highly reliable labels.

We evaluated multiple sampling ratios (2%, 10%, 50%, 66%, and 100%) to understand the trade-off between sample reliability and diversity. Empirically, 50–100% sampling offered the best balance, while extremely low ratios reduced coverage.

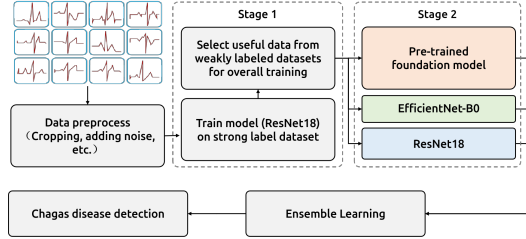


Figure 1. Overview of the Model Framework.

2.3. Model Architectures

Three models were trained independently to capture complementary representations of the electrocardiogram (ECG) signals, the model structure is shown in Figure 1:

- **Foundation Model:** The ECG foundation model was constructed using over ten million 12-lead electrocardiogram recordings from more than one million patients, annotated with 150 diagnostic labels [9]. A RegNet-based architecture was adopted to capture both temporal dynamics and spatial correlations across leads. The model was trained with a multilabel classification objective and included strategies to handle incomplete annotations and improve robustness. In addition, single-lead augmentation was incorporated to enhance adaptability for wearable and mobile applications, yielding expert-level performance across diverse diagnostic tasks and providing a versatile backbone for downstream use. Building on this foundation, we performed full fine-tuning of the network using our curated high-confidence dataset. Both the backbone parameters and the classification layer were updated during training, enabling the model to better adapt to the specific task of Chagas disease detection.

- **EfficientNet-B0:** A compact convolutional neural network (CNN) optimized for parameter efficiency [10]. We adapted this architecture for one-dimensional physiological signals by replacing image-based convolutions with temporal convolutions, allowing the model to extract multi-scale temporal features with minimal computational cost.

- **ResNet-18:** A residual CNN architecture [11] that facilitates gradient propagation through shortcut connections. We employed this network both as a baseline for model comparison and as a robust classifier for sample selection and downstream prediction.

2.4. Training Strategy

All the high-confidence samples were used to train the three models in the second stage. All models were trained with binary cross-entropy loss. The Adam optimizer was used with learning rate 10^{-3} , and a ReduceLROnPlateau scheduler adjusted the rate dynamically. Mini-batch size

was 64–512 depending on GPU memory. To improve generalization, we applied the following augmentations:

- Random cropping within the 10-s window.
- Lead masking, where 1–2 channels were randomly dropped.
- Amplitude scaling, multiplying signals by factors between 0.9 and 1.1.

For downstream adaptation, we fine-tuned the ECG foundation model on three distinct categories of curated high-confidence datasets, allowing the network to adjust its representations to the specific distributions of Chagas-related signals.

2.5. Fusion Strategy

While each model demonstrates strong performance individually, their error patterns and feature representations differ, suggesting potential gains from combining their outputs. Inspired by recent ensemble learning studies [12], we designed a fusion strategy for the ECG foundation model, EfficientNet-B0 and ResNet-18. Specifically, we assigned the same weights to the three models in the aggregation process and used the auxiliary models to refine decision boundaries and reduce model-specific variance. This foundation model-guided ensemble leverages the strong generalization ability of the pretrained backbone while incorporating the diversity of lightweight CNNs, resulting in improved robustness and stability across folds. For inference, we applied the fusion to obtain the weighted probabilities.

3. Results

Table 1 summarizes our results. The baseline ResNet-18 trained on 10% CODE-15% samples without demographic information achieved a cross-validation (CV) score of 0.308 and 0.310 on the training and hidden validation set respectively, demonstrating limited predictive capacity when trained with restricted data. Incorporating demographic features (e.g., age and sex) and increasing the proportion of training data provided modest improvements, with scores rising to 0.355 under a 50% sampling regime. These results suggest that demographic priors contain complementary information, but their contribution alone is not sufficient to close the performance gap.

In contrast to shallow baselines, strategies that leveraged high-confidence sampling and pretrained representation models consistently demonstrated superior performance. In particular, our standalone ECG foundation model achieved a Challenge score of 0.379 on the hidden validation set and a Challenge score of 0.238 on the test set, securing 10th place on the final leaderboard. This result highlights the strong transferability of foundation-model-based representations for clinical ECG signals,

Model	Training	Validation	Test
ResNet-s10	0.308	0.310	–
ResNet-s50-d	0.355	0.333	–
ResNet-2stage	0.371	–	–
EfficientNet-2stage	0.393	0.326	–
ECGFounder-2stage	0.391	0.379	0.238
Fusion	0.400	0.368	–

Table 1. Challenge scores for team MIWEAR across different model configurations. Training scores are obtained by 5-fold cross-validation (CV) on the public training data. Validation scores correspond to the official hidden validation set. Test scores and final rankings will be updated after the conference. ResNet-s10 indicates ResNet-18 trained with 10% randomly sampled CODE-15% data. ResNet-s50-d includes 50% sampled CODE-15% data with demographics. “2stage” refers to high-confidence sampling with a two-stage training scheme. ECGFounder-2stage denotes models initialized from ECG pretraining. Fusion (Confusion-2stage) indicates a weighted ensemble of multiple two-stage models.

even when trained under conditions of noisy labels and dataset heterogeneity. The foundation model’s robustness suggests that large-scale pretraining captures fundamental electrophysiological patterns that can be effectively adapted to downstream diagnostic tasks.

Beyond single models, we investigated ensemble learning as a means to further improve generalization. A fusion model guided by the ECG foundation model achieved the highest observed Challenge score of 0.400 on the training set, surpassing all individual models in terms of peak accuracy. The fusion design integrated predictions from diverse architectures while assigning dominant weight to the ECG foundation model, thereby preserving its discriminative capacity while exploiting complementary inductive biases from other networks. Although the ensemble did not outperform the standalone foundation model on the hidden validation set, it exhibited improved robustness across cross-validation folds and reduced susceptibility to model-specific overfitting.

4. Discussion and Conclusions

Our findings highlight several key insights regarding robust Chagas disease detection from ECG signals. First, confidence-based sample selection proved to be an effective strategy for mitigating label noise in large-scale heterogeneous ECG datasets. By emphasizing samples with higher predictive certainty, the model training became more stable and less influenced by mislabeled data. This observation is consistent with prior evidence showing that sample reweighting or confidence-based filtering improves robustness under label noise [13].

Second, the pretrained ECG foundation model substantially improved robustness compared with networks trained from scratch. Its strong transferability under distribution shifts suggests that large-scale pretraining captures general electrophysiological representations that remain useful across diverse cohorts, consistent with findings by Li et al. [9]. This mirrors trends observed in broader biomedical signal modeling, where foundation-scale pretraining leads to strong cross-dataset generalization [14].

Third, ensembling different architectures enhanced model stability but did not always improve peak hidden-validation performance. This reflects a classic bias-variance trade-off often reported in ensemble-based ECG classification. Our uniform averaging scheme improved robustness across folds but may have diluted the contribution of the strongest single model. Future work should explore adaptive weighting, calibration-based fusion, or uncertainty-aware aggregation [15] to balance robustness and accuracy more effectively.

This study has several limitations. The thresholds used for confidence-based selection were heuristic and may introduce selection bias. Restricting to high-confidence subsets reduces label noise but may also limit coverage of rare or atypical patterns. Moreover, the ensemble design was intentionally simple, and more advanced meta-ensemble or calibration methods could further improve generalization.

In conclusion, the combination of foundation-model pretraining, confidence-guided data curation, and model fusion provides a practical and effective framework for ECG-based disease detection. These components jointly enhance reliability under noisy supervision and domain shift, representing a generalizable strategy for other large-scale biomedical signal classification tasks.

Acknowledgments

The authors declare that they have no conflict of interest.

References

- [1] Goldberger AL, Amaral LA, Glass L, Hausdorff JM, Ivanov PC, Mark RG, et al. PhysioBank, PhysioToolkit, and PhysioNet: Components of a new research resource for complex physiologic signals. *Circulation* 2000;101(23):e215–e220.
- [2] Reyna MA, Koscova Z, Pavlus J, Weigle J, Saghafi S, Gomes P, et al. Detection of Chagas Disease from the ECG: The George B. Moody PhysioNet Challenge 2025. In Computing in Cardiology 2025, volume 52. 2025; 1–4.
- [3] Reyna MA, Koscova Z, Pavlus J, Saghafi S, Weigle J, Elola A, et al. Detection of Chagas Disease from the ECG: The George B. Moody PhysioNet Challenge 2025, 2025. URL <https://arxiv.org/abs/2510.02202>. DOI: 10.48550/arXiv.2510.02202.
- [4] Ribeiro A, Ribeiro M, Paixão G, Oliveira D, Gomes P, Canazart J, et al. Automatic diagnosis of the 12-lead ecg using a deep neural network. *Nature Communications* 2020; 11(1):1760.
- [5] Cardoso C, Sabino E, Oliveira C, de Oliveira L, Ferreira A, Cunha-Neto E, et al. Longitudinal study of patients with chronic chagas cardiomyopathy in brazil (SaMi-Trop project): a cohort profile. *BMJ Open* 2016;6(5):e0011181.
- [6] Wagner P, Strodtthoff N, Bousseljot RD, Kreiseler D, Lunze FI, Samek W, et al. PTB-XL, a large publicly available electrocardiography dataset. *Scientific Data* 2020;7:154.
- [7] Nunes M, Buss L, Silva J, Martins L, Oliveira C, Cardoso CS BB, et al. Incidence and predictors of progression to chagas cardiomyopathy: Long-term follow-up of trypanosoma cruzi-seropositive individuals. *Circulation* 2021; 144(19):1553–1566.
- [8] Pinto-Filho M, Brant L, Dos Reis R, Giatti L, Duncan B, Lotufo P, et al. Prognostic value of electrocardiographic abnormalities in adults from the brazilian longitudinal study of adults' health. *Heart* 2021;107(19):1560–1566.
- [9] Li J, Aguirre AD, Junior VM, Jin J, Liu C, Zhong L, et al. An electrocardiogram foundation model built on over 10 million recordings. *NEJM AI* 2025;2(7):A1oa2401033.
- [10] Tan M, Le Q. Efficientnet: Rethinking model scaling for convolutional neural networks. In International Conference on Machine Learning. PMLR, 2019; 6105–6114.
- [11] He K, Zhang X, Ren S, Sun J. Deep residual learning for image recognition. In Proceedings of the IEEE Conference on Computer Vision and Pattern Recognition. 2016; 770–778.
- [12] Wu W, Tan Y. Melicientnet: Harnessing mel-spectrograms and efficientnet architectures for predicting neurological recovery post-cardiac arrest. In 2023 Computing in Cardiology (CinC), volume 50. IEEE, 2023; 1–4.
- [13] Northcutt CG, Jiang L, Chuang IL. Confident learning: Estimating uncertainty in dataset labels. *Journal of Artificial Intelligence Research* 2021;70:1373–1411.
- [14] Rajpurkar P, Chen E, Banerjee O, Topol EJ. Deep learning for electrocardiogram interpretation: Review, opportunities, and challenges. *Nature Reviews Cardiology* 2022; 19(11):710–730.
- [15] Lakshminarayanan B, Pritzel A, Blundell C. Simple and scalable predictive uncertainty estimation using deep ensembles. *Advances in Neural Information Processing Systems* 2017;30.

Address for correspondence:

Wenlong Wu

33 Xi'erqi Middle Road, Haidian District, Beijing, China
wuwenlong3@xiaomi.com